THE EFFECT OF PARTICLE SHAPE AND STIFFNESS ON THE CONSTITUTIVE BEHAVIOR OF METAL-MATRIX COMPOSITES

Guoan Li

Orthopaedic Biomechanics Laboratory, School of Medicine, The Johns Hopkins University, Baltimore, MD 21205, U.S.A.

and

P. Ponte Castañeda

Department of Mechanical Engineering and Applied Mechanics, University of Pennsylvania, 220 Towne Building, 220 S. 33rd Street, Philadelphia, PA 19104, U.S.A.

Abstract—This paper deals with the *effective* constitutive behavior of ductile metals reinforced by aligned spheroidal inclusions with linear-elastic properties. For simplicity, both the matrix and the inclusions are assumed to be incompressible and isotropic, so that the overall constitutive behavior of the metal-matrix composites is incompressible and transversely isotropic. Based on a recently proposed variational method for estimating the effective behavior of nonlinear composites, results are obtained for the initial yield surfaces and overall stress–strain relations in terms of the three essentially distinct loading modes for this class of composites: Axisymmetric tension (relative to the symmetry axis of the inclusions), longitudinal shear (along the symmetry axis) and transverse shear (perpendicular to the symmetry axis). It is found that particle shape has a significant effect on the effective response of the composites, and that this effect is markedly different for the three loading modes. For the axisymmetric mode, oblate and prolate shapes have the largest strengthening effects; for the transverse mode, oblate shapes are most effective; and for the longitudinal mode, nearly spherical shapes are best. Particle stiffness also has a strong effect on the initial yielding behavior of the composites, which is magnified for the more severe aspect ratios. On the other hand, the stiffness of the particles does not seem to significantly affect the stress-strain behavior of the composites for strains greater than about five times the yield value.

1. INTRODUCTION

Because of potential applications to a number of technologically important problems, there has been over the past few years great interest in the problem of estimating the effective constitutive behavior of metal-matrix composites reinforced by stiff brittle particles. However, consideration of this fundamental problem dates back to the pioneering work of Drucker (1965, 1966), who estimated the effect of rigid particles on the effective yield strength of particle-reinforced composites with a perfectly plastic matrix. More recently, Duva (1984) made use of the numerical solution to a kernel problem for a rigid spherical particle in an infinite matrix of a power-law material, together with a differential self-consistent scheme, to estimate the effective behavior of the corresponding particle-reinforced composites. Similar analyses for power-law materials reinforced by aligned rigid spheroidal inclusions have been carried out by He (1990) and Lee and Mear (1991a, b), under axisymmetric loading conditions (relative to the symmetry axis of the inclusion). An alternative approach to the problem is to assume *periodic* microstructures, and to estimate the effective behavior in terms of solutions to boundary value problems, defined over unit cells of the microstructures, with periodic boundary conditions. This approach was taken by Christman *et al.* (1989), Tvergaard (1990) and Bao *et al.* (1991) for both spheroidal and cylindrical particles, under the simplifying assumptions of cylindrical unit cells and *axisymmetric* loading conditions (to achieve numerical simplicity). The first of these references also includes experimental results for a model SiC whisker-reinforced aluminum alloy. In addition, full three-dimensional finite element analyses were carried out by Hom (1992) for composites with cubic symmetry subjected to tension along and transverse to the alignment axis. It was found that all the above periodic calculations are in reasonably good agreement with each other, but they tend to overestimate the load-carrying capacity of the model experiments. We also note that Accorsi and Nemat-Nasser (1986) and Teply and Dvorak (1988) have developed methods for bounding the incremental stiffness tensors of periodic

composites, which may be used iteratively to obtain estimates for their overall stress–strain relations.

In this paper, we make use of an altogether different approach that, while lacking the accuracy and some of the features of the above mentioned analyses, possesses some distinct advantages of its own, including *simplicity* of application to *general* nonlinear behavior and loading conditions. This approach is based on a variational statement recently developed by Ponte Castañeda (1991a, 1992), which serves to determine the effective behavior of a given *nonlinear* composite in terms of the effective behavior of a certain class of *linear comparison* composites. This allows the application of the variational procedure to generate bounds and estimates for the effective behavior of classes of nonlinear composites in terms of bounds and estimates for corresponding classes of linear composites. Although many different types of bounds and estimates are possible on account of the existing wealth of results for linear-elastic composites, thus far the method has been applied mostly to obtain bounds and estimates of the Hashin–Shtrikman (1962, 1963) type. In this connection, it is important to point out that there is an older, different method, proposed by Talbot and Willis (1985), that also leads to bounds of the Hashin–Shtrikman (HS) type for nonlinear composites [see, for example, Willis (1991)]. Under certain technical assumptions that will be met in this paper, it can be shown that both methods yield the same HS *lower* bounds for the strain potential functions of nonlinear composites with isotropic phases. However, these bounds turn out to be of little practical value in the present work because they can be shown to correspond to "particulate" microstructures with the stiffer material playing the role of the matrix phase. Instead, estimates for the corresponding upper bounds will be used (which have not been obtained directly from the Talbot–Willis method). As discussed by Ponte Castañeda (1991b, 1992), these "upper estimates" for the strain potentials may be interpreted as estimates for the effective response of two-phase composites with particulate microstructures, such that the weaker phase plays the role of the matrix (as is the case for the metal-matrix composites of interest in this work). Finally, we note that a third approach, that is useful for very special classes of composites (essentially pure-power materials), was proposed recently by Suquet (1992a, b, 1993). However, it can be shown that this approach is entirely equivalent to the approach of Ponte Castañeda (PC), specialized to pure-power composites.

Application of these variational methods to obtain explicit estimates for the effective behavior of metal-matrix composites reinforced by rigid and elastic spherical inclusions were given respectively by Ponte Castañeda and Willis (1988) (self-consistent estimates using the Talbot–Willis method) and by Ponte Castañeda (1991a, b) (self-consistent and HS estimates using the PC method). Extensions of these results for composites reinforced by rigid spheroidal inclusions (using the PC method) were given by Talbot and Willis (1992) and by Li et al. (1993) [see also results of Suquet (1992a) for power-law materials]. The present paper generalizes these studies further by considering the effect of particle stiffness, in addition to the effects of particle concentration and shape. One difference in the approach of this paper from that followed for the corresponding periodic calculations discussed previously is that the arrangement of the particles within the composite cannot be controlled. This is because we will make use of the HS bounds of Willis (1977) for linear composites with "overall ellipsoidal symmetry" in the context of the PC variational procedure. In particular, this means that the results of this paper will not only apply to composites with aligned spheroidal inclusions, but more generally to any composite with equivalent overall symmetry [see Willis (1981)]. We conclude this section by noting that different estimates have also been obtained by Zhao and Weng (1990) for metal-matrix composites reinforced by aligned spheroidal inclusions; these are based on a framework developed earlier by Tandon and Weng (1988), which in turn consisted of an appropriate adaptation of the mean-field method of Mori and Tanaka (1973).

2. VARIATIONAL CHARACTERIZATION OF EFFECTIVE PROPERTIES

We consider a general specimen of a nonlinear heterogeneous material occupying a domain Ω (of unit volume) with boundary $\partial\Omega$. The material is characterized by a stress

potential $U(\mathbf{x}, \boldsymbol{\sigma})$, depending on position $\mathbf{x}$ and on the stress $\boldsymbol{\sigma}$, and such that the strain ε is given by

$$\varepsilon(\mathbf{x}) = \frac{\partial U(\mathbf{x}, \boldsymbol{\sigma})}{\partial \boldsymbol{\sigma}}. \tag{1}$$

Such a model provides an adequate characterization of the time-independent nonlinear constitutive behavior of ductile materials subjected to approximately proportional, quasi-static loading conditions [in the so-called context of deformation theory of plasticity; see Budiansky (1959)]. Alternatively, letting ε denote the strain-rate in the material, the above model is often used to characterize the high-temperature creeping behavior of metals.

Defining [see Hill (1963)] the effective potential function of the heterogeneous material by

$$\tilde{U}(\bar{\boldsymbol{\sigma}}) = \min_{\boldsymbol{\sigma} \in S(\bar{\boldsymbol{\sigma}})} \int_{\Omega} U(\mathbf{x}, \boldsymbol{\sigma}) \, dv, \tag{2}$$

where

$$S(\bar{\boldsymbol{\sigma}}) = \{ \boldsymbol{\sigma} | \nabla \cdot \boldsymbol{\sigma} = 0 \text{ in } \Omega, \quad \text{and} \quad \boldsymbol{\sigma} \mathbf{n} = \bar{\boldsymbol{\sigma}} \mathbf{n}, \; \mathbf{x} \in \partial \Omega \} \tag{3}$$

represents the set of statically admissible stress fields satisfying a uniform traction boundary condition, the effective constitutive relation for the heterogeneous material may then be given in terms of the relation

$$\bar{\varepsilon} = \frac{\partial \tilde{U}(\bar{\boldsymbol{\sigma}})}{\partial \bar{\boldsymbol{\sigma}}}, \tag{4}$$

where $\bar{\varepsilon}$ and $\bar{\boldsymbol{\sigma}}$ are the mean values of the strain and stress fields over Ω.

While the effective behavior of the composite is fully described by $\tilde{U}$ in terms of relation (4), the determination of $\tilde{U}$ from (2) and (3) presents real difficulties in that it requires the solution of a nonlinear boundary value problem with complex structure. Ponte Castañeda (1991a, 1992) introduced a variational principle that can be used to estimate the effective potential functions of nonlinear composites in terms of optimization problems involving the effective potential functions of appropriate classes of *linear* comparison composites. Thus, results for the effective properties of linear composites may be used to generate corresponding estimates for the effective properties of nonlinear composites. In this paper, we make use of the Hashin–Shtrikman bounds of Willis (1977, 1981) for linear composites with aligned spheroidal inclusions (or, more generally, with "ellipsoidal" two-point correlation functions) to estimate the effective constitutive behavior of ductile-matrix materials reinforced by aligned spheroidal inclusions with linear-elastic properties. The PC variational principle is briefly reviewed in the following.

For simplicity, we consider only composites with incompressible, isotropic phases. Thus, the potential function for the nonlinear heterogeneous material may be written in the form $U(\mathbf{x}, \boldsymbol{\sigma}) = \phi(\mathbf{x}, \tau_e)$, where $\tau_e = \sqrt{\frac{1}{2} \boldsymbol{\sigma}' \cdot \boldsymbol{\sigma}'}$ is the effective shear stress, and $\boldsymbol{\sigma}' = \boldsymbol{\sigma} - \sigma_m \mathbf{I}$ is the deviatoric stress tensor. (Note that the potential function ϕ is independent of the hydrostatic stress $\sigma_m = \text{tr} \, \boldsymbol{\sigma}/3$.) Then, under certain technical hypotheses [see Ponte Castañeda (1992)] satisfied in this paper, we may express the material potential function in terms of the optimization problem

$$U(\mathbf{x}, \boldsymbol{\sigma}) = \max_{\mu_0 \geqslant 0} \{ U_0(\mathbf{x}, \boldsymbol{\sigma}) - V(\mathbf{x}, \mu_0) \}, \tag{5}$$

where U_0 is the potential function of an incompressible, isotropic linear-elastic *comparison* material with variable shear modulus $\mu_0(\mathbf{x})$, such that $U_0(\mathbf{x}, \boldsymbol{\sigma}) = 1/(2\mu_0(\mathbf{x})) \tau_e^2$, and where

$$V(\mathbf{x}, \mu_0) = \max_{\sigma} \{U_0(\mathbf{x}, \sigma) - U(\mathbf{x}, \sigma)\}. \tag{6}$$

The variational principle follows by averaging the local relation (5) to give [see Ponte Castañeda (1992) for details]

$$\tilde{U}(\bar{\sigma}) = \max_{\mu_0(\mathbf{x}) \geqslant 0} \left\{ \tilde{U}_0(\bar{\sigma}) - \int_{\Omega} V(\mathbf{x}, \mu_0(\mathbf{x})) \, dv \right\}, \tag{7}$$

where

$$\tilde{U}_0(\bar{\sigma}) = \min_{\sigma \in S(\bar{\sigma})} \int_{\Omega} U_0(\mathbf{x}, \sigma) \, dv$$

is the effective potential of the linear comparison composite.

Relation (7) is an exact expression for the effective potential function of a given nonlinear composite, but it involves an infinite-dimensional optimization problem over the set of non-negative functions $\mu_0(\mathbf{x})$, and is therefore difficult to implement, except for some special types of microstructures [e.g. laminated composites; see deBotton and Ponte Castañeda (1992)]. However, it may be shown that (7) can be used in an approximate fashion to generate bounds for the effective properties of classes of nonlinear composites with more general microstructures. This will be done here in the context of two-phase composites.

The phases are assumed to be incompressible, isotropic and homogeneous, characterized by convex potential functions $U^{(r)}(\sigma) = \phi^{(r)}(\tau_e)$, with $r = 1$ and 2 corresponding to phases 1 and 2, respectively. Perfect bonding between phases is assumed, so that the effect of imperfections, in the form of micro-cracks and voids at the interfaces, is neglected. Further, the volume fractions of the phases, denoted by $c^{(r)}$ ($c^{(1)} + c^{(2)} = 1$), are also assumed to be known. Even then, the effective potential function given by (7) requires the solution of an infinite-dimensional optimization problem over the set of functions $\mu_0(\mathbf{x})$. However, by restricting our attention to the class of piecewise constant $\mu_0(\mathbf{x})$ (constant in each phase of the nonlinear material), we arrive at the following lower bound approximation for the effective potential function of the nonlinear composite, namely,

$$\tilde{U}(\bar{\sigma}) \geqslant \max_{\mu_0^{(1)}, \mu_0^{(2)} \geqslant 0} \left\{ \tilde{U}_0(\bar{\sigma}) - \sum_{r=1}^{2} c^{(r)} V^{(r)}(\mu_0^{(r)}) \right\}, \tag{8}$$

where $\mu_0^{(1)}$ and $\mu_0^{(2)}$ are the values of $\mu_0(\mathbf{x})$ in phases 1 and 2, respectively. Also, $\tilde{U}_0(\bar{\sigma})$ now corresponds to the effective potential function of a linear comparison composite with *precisely* the same microstructure as the nonlinear composite, and

$$V^{(r)}(\mu_0^{(r)}) = \max_{\tau_e} \left\{ \frac{1}{2\mu_0^{(r)}} \tau_e^2 - \phi^{(r)}(\tau_e) \right\}. \tag{9}$$

For later reference, we note that [cf. eqn (6)]

$$\phi^{(r)}(\tau_e) = \max_{\mu_0^{(r)}} \left\{ \frac{1}{2\mu_0^{(r)}} \tau_e^2 - V^{(r)}(\mu_0^{(r)}) \right\}. \tag{10}$$

The optimization problem implied by (8) is two-dimensional, and therefore simpler to solve than that implied by (7), provided that we have estimates for the effective potential of the relevant two-phase, linear comparison composite. In addition, if we have a lower bound for the effective potential $\tilde{U}_0$ of a given class of linear comparison composites, then (8) generates a lower bound for the effective potential $\tilde{U}$ of the corresponding class of nonlinear

composites. If, on the other hand, we have an upper bound for $\tilde{U}_0$, then (8) will not necessarily generate an upper bound for $\tilde{U}$; instead, it will generate only an estimate for $\tilde{U}$. Such an estimate will be referred to in this paper as an "upper estimate" to distinguish it from the lower bound.

As mentioned previously, in this paper, we will make use of *Hashin–Shtrikman upper bounds* for the strain potential $\tilde{U}_0$ of the linear comparison composites to generate corresponding *upper estimates* for the nonlinear metal-matrix composites. There are good reasons for this approach. First, it has been shown by Francfort and Murat (1986) that the Hashin–Shtrikman (1963) bounds for linear composites with isotropic overall symmetry are attainable by special types of "particulate" microstructures with clearly defined matrix and inclusion phases. Thus, the upper (lower) bound for $\tilde{U}_0$ is attained by microstructures with the stiffer material occupying the inclusion (matrix) phase and the more compliant material in the matrix (inclusion) phase. Analogous results have been shown by Lipton (1991) for the HS bounds of Hill (1964) and Hashin (1965) for fiber-reinforced composites with transversely isotropic overall symmetry, and it is likely that similar results could be proved for the bounds of Willis (1977) for composites with "ellipsoidal" overall symmetries. Therefore, it makes sense to regard the bounds of Willis as reasonable estimates for composites with particulate microstructures, where the inclusion shape is ellipsoidal. In fact, Willis (1980, 1981) has shown that the expressions for the bounds of Willis (1977) for composites with ellipsoidal symmetry actually constitute variational estimates for the effective moduli of composites containing aligned ellipsoids. In our problem, we are interested in metal-matrix composites reinforced by aligned spheroidal inclusions with linear properties. It is then consistent with the previous remarks for linear composites, to regard the nonlinear estimates for $\tilde{U}$, obtained via (8), from the HS upper bounds of Willis for $\tilde{U}_0$, as sensible estimates for the effective behavior of metal-matrix composites consisting of a relatively compliant matrix phase, reinforced by stiffer linear-elastic inclusions. The second reason for using the bounds of Willis (1977) is that their analytic expressions are considerably simpler than the corresponding expressions for other types of estimates, such as self-consistent (Budiansky, 1965; Hill, 1965) and generalized self-consistent estimates (Christensen and Lo, 1979). This leads to significant simplification in the context of making use of the variational statement (8).

3. NONLINEAR INCOMPRESSIBLE COMPOSITES REINFORCED WITH ALIGNED SPHEROIDAL INCLUSIONS

In this section, we consider the application of the above procedure to the class of two-phase composites with nonlinear, incompressible matrices reinforced by aligned, nonlinear, incompressible spheroidal inclusions. In the next section, we will consider the specialization of these results to metal-matrix composites reinforced by linear-elastic inclusions. The aspect ratio of the inclusions is given by $\alpha = b/a$, where a and b are defined in Fig. 1, so that $\alpha < 1$ and $\alpha > 1$ correspond to oblate and prolate inclusions, respectively. We let materials 1 and 2 correspond to the matrix and inclusion phases, so that $U^{(1)}(\boldsymbol{\sigma}) = \phi^{(1)}(\tau_e)$, $U^{(2)}(\boldsymbol{\sigma}) = \phi^{(2)}(\tau_e)$ and $c^{(1)}, c^{(2)}$ denote the stress potentials and volume fractions of the matrix and inclusion phases, respectively. We note that, while each phase of the composite is isotropic, the geometrical arrangement of the inclusions results in overall transversely isotropic symmetry for the composite. In the following subsection, we recall the results of Willis (1977) for the linear-elastic comparison composites, which will be used in later sections to obtain estimates for the effective potential and stress–strain relations of the nonlinear composites just described.

3.1. Linear comparison composites

The geometry of the linear-elastic composites considered in this subsection is precisely the same as that described above for the nonlinear composites. However, since the properties of the phases are linear, their behavior may be described in terms of fourth-order compliance tensors $M^{(r)}$ ($r = 1$ and 2, corresponding respectively to the matrix and inclusion phases).
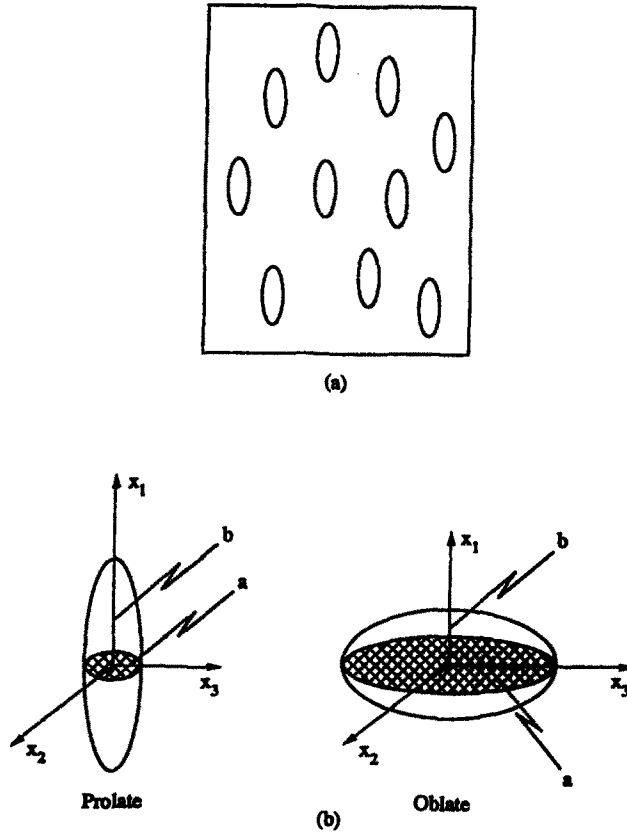
Fig. 1. (a) Composite materials reinforced by aligned spheroidal inclusions. (b) Geometry of prolate and oblate spheroids.

Because the phases are isotropic, these tensors depend only on two parameters each : The shear moduli $\mu_0^{(r)}$ and the bulk moduli $k_0^{(r)}$ of the two phases ($r = 1, 2$).

It then follows from the work of Willis (1977) [see also Walpole (1966, 1969), Willis (1980, 1981) and Weng (1992)] for linear composites with overall ellipsoidal symmetry, or analogously for linear composites reinforced by aligned ellipsoidal inclusions, that an estimate for the effective compliance tensor $\tilde{M}$ of the class of two-phase linear composites of interest here may be expressed in the form

$$\tilde{M}^{(e)} = \sum_{r=1}^{2} c^{(r)} M^{(r)} B(r) \left\{ \sum_{s=1}^{2} c^{(s)} B^{(r)} \right\}^{-1}, \tag{11}$$

where the $B^{(r)}$ ($r = 1, 2$) are the stress concentration tensors (Hill, 1965) of the two phases (associated with ellipsoidal inclusions embedded in infinite matrices), given by

$$B^{(r)} = [I + (M^{(0)})^{-1}(I - S^{(0)})(M^{(r)} - M^{(0)})]^{-1}. \tag{12}$$

In this last relation, $M^{(0)}$ denotes the compliance tensor of a homogeneous comparison material, I is the fourth-order identity tensor, and $S^{(0)}$ denotes the Eshelby (1957) tensor associated with an ellipsoidal inclusion embedded in a matrix with compliance tensor $M^{(0)}$. For the special case of a *spheroidal* inclusion embedded in an *isotropic* matrix, $S^{(0)}$ is transversely isotropic and may be expressed, in the notation of Walpole (1969), as

$$S^{(0)} = (S^{(0)}_{2222} + S^{(0)}_{2233}, S^{(0)}_{1111}, 2S^{(0)}_{2323}, 2S^{(0)}_{1212}, S^{(0)}_{1122}, S^{(0)}_{2211}), \qquad (13)$$

where the nonzero components of $S^{(0)}$ are given explicitly in Appendix A. In these expressions, x_1 denotes the direction of inclusion alignment (a symmetry axis), and x_2, x_3 are perpendicular to x_1 (see Fig. 1).

To obtain the required upper bound for the effective compliance $\tilde{M}$ (a lower bound for the stiffness) of the relevant class of linear composites, the compliance of the comparison material $M^{(0)}$ in (11) must be set equal to that of the less stiff phase $M^{(1)}$ (in this case the matrix phase). Then, after some algebra, (11) leads to an upper bound of the form

$$\tilde{M}^{(+)} = M^{(1)} + c^{(2)}[(M^{(2)}(M^{(1)})^{-1} - I)^{-1} + c^{(1)}(I - S^{(1)})]^{-1} M^{(1)}, \qquad (14)$$

where $S^{(1)}$ denotes the Eshelby tensor associated with phase 1. The resulting overall compliance tensor can be shown to be transversely isotropic, and may be simplified further, if the phases are incompressible (i.e. $k_0^{(r)} \to \infty$), to take the form

$$\tilde{M}^{(+)} = \left(\frac{1}{2\tilde{\mu}_d}, \frac{1}{\tilde{\mu}_d}, \frac{1}{2\tilde{\mu}_p}, \frac{1}{2\tilde{\mu}_n}, -\frac{1}{2\tilde{\mu}_d}, -\frac{1}{2\tilde{\mu}_d} \right), \qquad (15)$$

where $\tilde{\mu}_d$, $\tilde{\mu}_p$ and $\tilde{\mu}_n$ are given by

$$\frac{\mu_0^{(1)}}{\tilde{\mu}_d} = 1 - c^{(2)} \frac{1-\varepsilon}{1 - c^{(1)}(1-\varepsilon) f(\alpha)},$$

$$\frac{\mu_0^{(1)}}{\tilde{\mu}_p} = 1 - c^{(2)} \frac{1-\varepsilon}{1 - c^{(1)}(1-\varepsilon)(1 - 2S^{(1)}_{2323}(\alpha))},$$

$$\frac{\mu_0^{(1)}}{\tilde{\mu}_n} = 1 - c^{(2)} \frac{1-\varepsilon}{1 - c^{(1)}(1-\varepsilon)(1 - 2S^{(1)}_{1212}(\alpha))}, \qquad (16)$$

and correspond to the three independent shear moduli of the linear, incompressible, transversely isotropic composites. In this last relation, $\varepsilon = \mu_0^{(1)}/\mu_0^{(2)} (\leqslant 1)$ denotes the ratio of the shear modulus of matrix material to that of the inclusion, f is a function of the aspect ratio α, which is given explicitly in Appendix A, and $S^{(1)}_{2323}$ and $S^{(1)}_{1212}$ are the relevant components of the Eshelby tensor, which, for an incompressible matrix, are also only functions of the aspect ratio α.

We further note that the associated effective stress potential $\tilde{U}_0^{(+)}$ is given by [see Walpole (1969)]

$$\tilde{U}_0^{(+)}(\bar{\sigma}) = \frac{1}{2\tilde{\mu}_d} \bar{\tau}_d^2 + \frac{1}{2\tilde{\mu}_p} \bar{\tau}_p^2 + \frac{1}{2\tilde{\mu}_n} \bar{\tau}_n^2, \qquad (17)$$

where $\bar{\tau}_d$, $\bar{\tau}_p$ and $\bar{\tau}_n$ are the three transversely isotropic invariants of the applied stress tensor $\bar{\sigma}$, corresponding to the three independent loading modes of an incompressible, transversely isotropic material: Axisymmetric deviatoric stress (relative to the symmetry axis), transverse shear stress (in the plane perpendicular to the symmetry axis) and longitudinal shear stress (along the symmetry axis), respectively. In components, these stress invariants are given by

$$\bar{\tau}_d = \frac{1}{\sqrt{3}}[\tfrac{1}{2}(\bar{\sigma}_{33} + \bar{\sigma}_{22}) - \bar{\sigma}_{11}],$$

$$\bar{\tau}_p = [\bar{\sigma}_{23}^2 + \tfrac{1}{4}(\bar{\sigma}_{33} - \bar{\sigma}_{22})^2]^{1/2},$$

$$\bar{\tau}_n = (\bar{\sigma}_{12}^2 + \bar{\sigma}_{13}^2)^{1/2}, \qquad (18)$$

and can be shown to be related to the average equivalent shear stress $\bar{\tau}_e$ through

$$\bar{\tau}_e = (\bar{\tau}_d^2 + \bar{\tau}_p^2 + \bar{\tau}_n^2)^{1/2}. \tag{19}$$

Next, making use of the following identity introduced by deBotton and Ponte Castañeda (1992),

$$\left(\sum_{r=1}^{2} c^{(r)} \mu^{(r)}\right)^{-1} = \min_{\omega} \left\{ \frac{c^{(1)}}{\mu^{(1)}} [1 + c^{(2)}\omega]^2 + \frac{c^{(2)}}{\mu^{(2)}} [1 - c^{(1)}\omega]^2 \right\}, \tag{20}$$

we are able to derive the following expressions for the three effective moduli of (16), namely,

$$\frac{1}{\tilde{\mu}_d} = \min_{\omega} \left\{ \frac{Q_d^{(1)}}{\mu_0^{(1)}} + \frac{Q_d^{(2)}}{\mu_0^{(2)}} \right\},$$

$$\frac{1}{\tilde{\mu}_p} = \min_{\beta} \left\{ \frac{Q_p^{(1)}}{\mu_0^{(1)}} + \frac{Q_p^{(2)}}{\mu_0^{(2)}} \right\},$$

$$\frac{1}{\tilde{\mu}_n} = \min_{\gamma} \left\{ \frac{Q_n^{(1)}}{\mu_0^{(1)}} + \frac{Q_n^{(2)}}{\mu_0^{(2)}} \right\}, \tag{21}$$

where

$$Q_d^{(1)}(\omega) = 1 + c^{(2)} \left[\frac{c^{(1)}[1 - c^{(2)}\omega]^2}{f(\alpha)} - (c^{(2)})^2 [1 + c^{(1)}\omega]^2 \right],$$

$$Q_p^{(1)}(\beta) = 1 + c^{(2)} \left[\frac{c^{(1)}[1 - c^{(2)}\beta]^2}{1 - 2S_{2323}^{(1)}(\alpha)} - (c^{(2)})^2 [1 + c^{(1)}\beta]^2 \right],$$

$$Q_n^{(1)}(\gamma) = 1 + c^{(2)} \left[\frac{c^{(1)}[1 - c^{(2)}\gamma]^2}{1 - 2S_{1212}^{(1)}(\alpha)} - (c^{(2)})^2 [1 + c^{(1)}\gamma]^2 \right], \tag{22}$$

and

$$Q_d^{(2)}(\omega) = (c^{(2)})^3 [1 + c^{(1)}\omega]^2,$$

$$Q_p^{(2)}(\beta) = (c^{(2)})^3 [1 + c^{(1)}\beta]^2,$$

$$Q_n^{(2)}(\gamma) = (c^{(2)})^3 [1 + c^{(1)}\gamma]^2. \tag{23}$$

As a consequence of these relations, the upper bound $\tilde{U}_0$ for the effective stress potential in (17) may be expressed in the form

$$\tilde{U}_0^{(+)}(\bar{\sigma}) = \min_{\omega,\beta,\gamma} \left\{ c^{(1)} \frac{(\bar{\tau}_e^{(1)})^2}{2\mu_0^{(1)}} + c^{(2)} \frac{(\bar{\tau}_e^{(2)})^2}{2\mu_0^{(2)}} \right\}, \tag{24}$$

where

$$\bar{\tau}_e^{(1)} = \frac{\sqrt{Q_d^{(1)}(\omega)\bar{\tau}_d^2 + Q_p^{(1)}(\beta)\bar{\tau}_p^2 + Q_n^{(1)}(\gamma)\bar{\tau}_n^2}}{\sqrt{c^{(1)}}}, \tag{25}$$

$$\bar{\tau}_e^{(2)} = \frac{\sqrt{Q_d^{(2)}(\omega)\bar{\tau}_d^2 + Q_p^{(2)}(\beta)\bar{\tau}_p^2 + Q_n^{(2)}(\gamma)\bar{\tau}_n^2}}{\sqrt{c^{(2)}}}. \tag{26}$$

We note that $\bar{\tau}_e^{(1)}$ and $\bar{\tau}_e^{(2)}$ may be thought of as estimates for the average equivalent shear stresses in the matrix and inclusion phases, respectively. However, these estimates are not

consistent, in general, with the estimates that may be obtained directly for the polarizations in the context of the Hashin–Shtrikman variational principles.

3.2. Nonlinear composites

With expression (24) for $\tilde{U}_0^{(+)}$ serving as an upper bound for the effective potentials of the linear comparison composites, we may obtain a corresponding upper estimate $\tilde{U}^{(+)}$ (not a rigorous bound) for the effective potentials of the nonlinear composites. This is accomplished by substituting (24) into (8) to obtain

$$\tilde{U}^{(+)}(\bar{\sigma}) = \max_{\mu_0^{(1)}, \mu_0^{(2)} > 0} \left\{ \min_{\omega,\beta,\gamma} \left\{ c^{(1)} \frac{(\bar{\tau}_e^{(1)})^2}{2\mu_0^{(1)}} + c^{(2)} \frac{(\bar{\tau}_e^{(2)})}{2\mu_0^{(2)}} \right\} - \sum_{r=1}^{2} c^{(r)} V^{(r)}(\mu_0^{(r)}) \right\}. \tag{27}$$

By interchanging the order of the maxima and minima (as allowed by the Saddle Point Theorem) above, and making use of relations (10), we arrive at the simple expression

$$\tilde{U}^{(+)}(\bar{\sigma}) = \min_{\omega,\beta,\gamma} \{ c^{(1)} \phi^{(1)}(\bar{\tau}_e^{(1)}) + c^{(2)} \phi^{(2)}(\bar{\tau}_e^{(2)}) \}, \tag{28}$$

where $\bar{\tau}_e^{(1)}$ and $\bar{\tau}_e^{(2)}$, which are functions of the applied mean stress $\bar{\sigma}$, as well as of ω, β and γ, are as given by (25) and (26), respectively. We further note that, in view of expression (28), $\bar{\tau}_e^{(1)}$ and $\bar{\tau}_e^{(2)}$ depend not only on the inclusion volume fraction and aspect ratio, but also on the constitutive properties of the matrix and inclusion phases (as characterized by the functional forms of $\phi^{(1)}$ and $\phi^{(2)}$).

Given the upper estimate (28) for the effective potential of nonlinear composites with aligned spheroidal inclusions of a stiffer material, we may compute the corresponding effective stress–strain relations for the composites in the usual fashion. To do this efficiently, it is useful to introduce the transversely isotropic invariants of the applied strain, corresponding to the stress invariants given in (19). They are the axisymmetric deviatoric strain $\bar{\gamma}_d$, the transverse shear strain $\bar{\gamma}_p$, and the longitudinal shear strain $\bar{\gamma}_n$. In components, they are given by

$$\bar{\gamma}_d = \frac{2}{\sqrt{3}} [\tfrac{1}{2}(\bar{\varepsilon}_{33} + \bar{\varepsilon}_{22}) - \bar{\varepsilon}_{11}],$$

$$\bar{\gamma}_p = 2[\bar{\varepsilon}_{23}^2 + \tfrac{1}{4}(\bar{\varepsilon}_{33} - \bar{\varepsilon}_{22})^2]^{1/2},$$

$$\bar{\gamma}_n = 2(\bar{\varepsilon}_{12}^2 + \bar{\varepsilon}_{13}^2)^{1/2}, \tag{29}$$

and they are related to the average equivalent shear strain $\bar{\gamma}_e = \sqrt{\bar{\varepsilon}' \cdot \bar{\varepsilon}'}$ through

$$\bar{\gamma}_e = (\bar{\gamma}_d^2 + \bar{\gamma}_p^2 + \bar{\gamma}_n^2)^{1/2}. \tag{30}$$

Then, the effective stress–strain relations for the particle-reinforced nonlinear composites are given by expressions

$$\bar{\gamma}_d = \frac{\partial \tilde{U}^{(+)}}{\partial \bar{\tau}_d}, \quad \bar{\gamma}_p = \frac{\partial \tilde{U}^{(+)}}{\partial \bar{\tau}_p}, \quad \bar{\gamma}_n = \frac{\partial \tilde{U}^{(+)}}{\partial \bar{\tau}_n}, \tag{31}$$

which, making use of (28) [see deBotton and Ponte Castañeda (1992)], may be rewritten in the form

$$\bar{\gamma}_d = \left(\frac{Q_d^{(1)}}{\bar{\tau}_e^{(1)}} \frac{\partial \phi^{(1)}}{\partial \bar{\tau}_e^{(1)}} + \frac{Q_d^{(2)}}{\bar{\tau}_e^{(2)}} \frac{\partial \phi^{(2)}}{\partial \bar{\tau}_e^{(2)}}\right)\bar{\tau}_d \Bigg|_{(\omega,\beta,\gamma) = (\hat{\omega},\hat{\beta},\hat{\gamma})},$$

$$\bar{\gamma}_p = \left(\frac{Q_p^{(1)}}{\bar{\tau}_e^{(1)}} \frac{\partial \phi^{(1)}}{\partial \bar{\tau}_e^{(1)}} + \frac{Q_p^{(2)}}{\bar{\tau}_e^{(2)}} \frac{\partial \phi^{(2)}}{\partial \bar{\tau}_e^{(2)}}\right)\bar{\tau}_p \Bigg|_{(\omega,\beta,\gamma) = (\hat{\omega},\hat{\beta},\hat{\gamma})},$$

$$\bar{\gamma}_n = \left(\frac{Q_n^{(1)}}{\bar{\tau}_e^{(1)}} \frac{\partial \phi^{(1)}}{\partial \bar{\tau}_e^{(1)}} + \frac{Q_n^{(2)}}{\bar{\tau}_e^{(2)}} \frac{\partial \phi^{(2)}}{\partial \bar{\tau}_e^{(2)}}\right)\bar{\tau}_m \Bigg|_{(\omega,\beta,\gamma) = (\hat{\omega},\hat{\beta},\hat{\gamma})}, \tag{32}$$

where $\bar{\tau}_e^{(1)}$ and $\bar{\tau}_e^{(2)}$ are given by (25) and (26), respectively, and where $\hat{\omega}$, $\hat{\beta}$, $\hat{\gamma}$ are the optimized values of ω, β, γ from (28), respectively. We emphasize that, in the above expressions, the derivatives may be evaluated keeping ω, β and γ fixed.

In summary, expression (28) for the effective potential $\tilde{U}^{(+)}$, and the corresponding stress–strain relations (32), serve to characterize the effective constitutive behavior of the class of two-phase nonlinear composites with aligned spheroidal inclusions (of a stiffer material) in terms of a simple three-dimensional optimization problem in the three variables ω, β and γ. The results apply for general inclusion volume fraction and aspect ratio, as well as for general applied loading conditions and general nonlinear (incompressible and isotropic) constitutive behavior for the matrix and inclusion phases. They generalize corresponding results for laminated composites ($\alpha = 0$) and fiber-reinforced composites ($\alpha = \infty$) by deBotton and Ponte Castañeda (1992, 1993), and for composites reinforced by rigid particles by Talbot and Willis (1992) and Li et al. (1993).

4. APPLICATION TO METAL-MATRIX COMPOSITES

In this section, we specialize the results of the previous section for general nonlinear, two-phase composites with spheroidal inclusions to metal-matrix composites reinforced by stiff linear-elastic inclusions. Thus, we will take the potential of the matrix phase to correspond to a linear/power-law material, and that of the inclusion phase to a linear-elastic material. In practice, as in the model metal-matrix composites used by Christman et al. (1988) (SiC whisker-reinforced aluminum alloys), both the matrix and the inclusion phases will exhibit compressible behavior. However, in this work, we will neglect the effect of compressibility; our goal will not be to accurately model any specific material system, but to explore in the simplest possible context the effects of particle shape and stiffness on overall behavior. The methods of this paper can be extended to include compressible (and even anisotropic) behavior for the constituent phases at the expense of complicating the analysis. This will be pursued elsewhere.

With the above limitations in mind, we choose the following uniaxial stress–strain relation [also used by Tvergaard (1990)] to characterize the behavior of the model matrix phases, namely,

$$\varepsilon = \begin{cases} \dfrac{\sigma}{E^{(1)}}, & \text{for } \sigma \leqslant \sigma_y^{(1)}, \\[12pt] \dfrac{\sigma_y^{(1)}}{E^{(1)}} \left(\dfrac{\sigma}{\sigma_y^{(1)}}\right)^n, & \text{for } \sigma > \sigma_y^{(1)}, \end{cases} \tag{33}$$

where $E^{(1)}$ is Young's modulus, $\sigma_y^{(1)}$ is the uniaxial yield stress and n is the strain-hardening exponent of the material. These relations can be generalized to multi-axial stress states via the expressions

$$\varepsilon' = \begin{cases} \dfrac{1}{2\mu^{(1)}} \sigma', & \text{for } \tau_e \leqslant \tau_y^{(1)}, \\[12pt] \dfrac{1}{2\mu^{(1)}} \left(\dfrac{\tau_e}{\tau_y^{(1)}}\right)^{n-1} \sigma', & \text{for } \tau_e > \tau_y^{(1)}, \end{cases} \tag{34}$$

where we have made use of the relation $E^{(1)} = 3\mu^{(1)}$ (with $\mu^{(1)}$ denoting the shear modulus

of phase 1) for an incompressible material, and where $\tau_y^{(1)} = \sigma_y^{(1)}/\sqrt{3}$ denotes the yield stress in shear of the matrix material.

The corresponding strain potential function may be obtained from

$$U^{(1)}(\sigma) = \int_0^{\sqrt{3}\tau_e} \varepsilon(\sigma) \cdot \mathrm{d}\sigma = \phi^{(1)}(\tau_e), \tag{35}$$

so that

$$\phi^{(1)}(\tau_e) = \frac{\tau_e^2}{2\mu^{(1)}} + \frac{(\tau_y^{(1)})^2}{2\mu^{(1)}} \left\{ \frac{2}{n+1} \left[\left(\frac{\tau_e}{\tau_y^{(1)}} \right)^{n+1} - 1 \right] - \left[\left(\frac{\tau_e}{\tau_y^{(1)}} \right)^2 - 1 \right] \right\} H(\tau_e - \tau_y^{(1)}), \tag{36}$$

where H is the Heaviside step function. Note that the material becomes linear in the limit as $n \to 1$, and elastic/perfectly plastic in the limit as $n \to \infty$.

On the other hand, the constitutive behavior of the linear-elastic inclusions is characterized by the quadratic potential

$$U^{(2)}(\sigma) = \phi^{(2)}(\tau_e) = \frac{\tau_e^2}{2\mu^{(2)}}, \tag{37}$$

where $\mu^{(2)}$ is the shear modulus of the inclusion material. For consistency with the assumptions of Section 3, we assume that $\mu^{(2)} \geqslant \mu^{(1)}$.

The effective stress potential of the composite material is thus obtained by substituting (36) and (37) into (28), which gives

$$\tilde{U}^{(+)}(\bar{\sigma}) = \min_{\omega,\beta,\gamma} \left\{ c^{(1)} \frac{(\bar{\tau}_e^{(1)})^2}{2\mu^{(1)}} + c^{(1)} \frac{(\tau_y^{(1)})}{2\mu^{(1)}} \left(\frac{2}{n+1} \left[\left(\frac{\bar{\tau}_e^{(1)}}{\tau_y^{(1)}} \right)^{n+1} - 1 \right] \right. \right.$$
$$\left. \left. - \left[\left(\frac{\bar{\tau}_e^{(1)}}{\tau_y^{(1)}} \right)^2 - 1 \right] \right) H(\bar{\tau}_e^{(1)} - \tau_y^{(1)}) + c^{(2)} \frac{(\bar{\tau}_e^{(2)})^2}{2\mu^{(2)}} \right\}, \tag{38}$$

where $\bar{\tau}_e^{(1)}$ and $\bar{\tau}_e^{(2)}$ are given by (25) and (26), respectively. Also, denoting, by $\hat{\omega}, \hat{\beta}, \hat{\gamma}$ the optimized values of ω, β, γ above, we obtain, from (32), the following expressions for the effective stress–strain relations of the composite

$$\frac{\bar{\gamma}_d}{\gamma_y^{(1)}} = \left\{ \left[1 + \left(\left(\frac{\bar{\tau}_e^{(1)}}{\tau_y^{(1)}} \right)^{n-1} - 1 \right) H(\bar{\tau}_e^{(1)} - \tau_y^{(1)}) \right] Q_d^{(1)}(\hat{\omega}) + Q_d^{(2)}(\hat{\omega}) \frac{\mu^{(1)}}{\mu^{(2)}} \right\} \frac{\bar{\tau}_d}{\tau_y^{(1)}},$$

$$\frac{\bar{\gamma}_p}{\gamma_y^{(1)}} = \left\{ \left[1 + \left(\left(\frac{\bar{\tau}_e^{(1)}}{\tau_y^{(1)}} \right)^{n-1} - 1 \right) H(\bar{\tau}_e^{(1)} - \tau_y^{(1)}) \right] Q_p^{(1)}(\hat{\beta}) + Q_p^{(2)}(\hat{\beta}) \frac{\mu^{(1)}}{\mu^{(2)}} \right\} \frac{\bar{\tau}_p}{\tau_y^{(1)}},$$

$$\frac{\bar{\gamma}_n}{\gamma_y^{(1)}} = \left\{ \left[1 + \left(\left(\frac{\bar{\tau}_e^{(1)}}{\tau_y^{(1)}} \right)^{n-1} - 1 \right) H(\bar{\tau}_e^{(1)} - \tau_y^{(1)}) \right] Q_n^{(1)}(\hat{\gamma}) + Q_n^{(2)}(\hat{\gamma}) \frac{\mu^{(1)}}{\mu^{(2)}} \right\} \frac{\bar{\tau}_n}{\tau_y^{(1)}}, \tag{39}$$

where $\bar{\tau}_e^{(1)}$ is evaluated at $\omega = \hat{\omega}$, $\beta = \hat{\beta}$ and $\gamma = \hat{\gamma}$, and where $\gamma_y^{(1)} = \sqrt{3}\varepsilon_y^{(1)}$ denotes the yield strain in shear of the matrix phase (here $\varepsilon_y^{(1)} = \sigma_y^{(1)}/E^{(1)}$ is the matrix yield strain in tension). These three expressions characterize the effective stress–strain relations for the three deformation modes of the transversely isotropic, incompressible particle-reinforced composite.

Because of the action of the Heaviside function H, in both expression (38) for the effective potential and expressions (39) for the effective stress–strain relations, we may interpret the function defined by

$$\Phi^{(+)}(\bar{\sigma}) = \bar{\tau}_e^{(1)}(\bar{\sigma})/\tau_y^{(1)} - 1, \tag{40}$$

with $\bar{\tau}_e^{(1)}$ evaluated at $\dot{\omega}$, $\hat{\beta}$ and $\hat{\gamma}$, as the effective yield function of the nonlinear composite. This function is such that $\Phi^{(+)}(\bar{\sigma}) < 0$ if the applied stress $\bar{\sigma}$ is within the elastic region of the composite, $\Phi^{(+)}(\bar{\sigma}) = 0$ at yield and $\Phi^{(+)}(\bar{\sigma}) > 0$ in the plastic range. Thus, this yield condition for the composite has the following physical interpretation: The composite yields when the "average equivalent shear stress" in the matrix phase $\bar{\tau}_e^{(1)}$ reaches its yield value $\tau_y^{(1)}$. This is expected to be *only* an approximation, but one that is consistent with the homogenization model used.

An alternative form for the yield function, valid only in the elastic range of the composite, may be obtained from (40) by solving for the optimal values of ω, β, γ in the *linear* range of the composite, and substituting these into $\bar{\tau}_e^{(1)}$ in (40). The result is

$$\Phi^{(+)}(\bar{\sigma}) = \sqrt{\left(\frac{\bar{\tau}_d}{(\bar{\tau}_y)_d}\right)^2 + \left(\frac{\bar{\tau}_p}{(\bar{\tau}_y)_p}\right)^2 + \left(\frac{\bar{\tau}_n}{(\bar{\tau}_y)_n}\right)^2} - 1, \tag{41}$$

where $(\bar{\tau}_y)_d$, $(\bar{\tau}_y)_p$ and $(\bar{\tau}_y)_n$ denote the effective yield stresses in the *pure* axisymmetric, transverse and longitudinal loading modes, respectively. They are given explicitly by

$$\frac{(\bar{\tau}_y)_d}{\tau_y^{(1)}} = \sqrt{c^{(1)}\left[1 - c^{(2)}\frac{1 - c^{(1)}f(\alpha)(1 - \mu^{(1)}/\mu^{(2)})^2}{(1 - c^{(1)}f(\alpha)(1 - \mu^{(1)}/\mu^{(2)}))^2}\right]^{-1}},$$

$$\frac{(\bar{\tau}_y)_p}{\tau_y^{(1)}} = \sqrt{c^{(1)}\left[1 - c^{(2)}\frac{1 - c^{(1)}(1 - 2S_{2323}^{(1)}(\alpha))(1 - \mu^{(1)}/\mu^{(2)})^2}{(1 - c^{(1)}(1 - \mu^{(1)}/\mu^{(2)})(1 - 2S_{2323}^{(1)}(\alpha)))^2}\right]^{-1}},$$

$$\frac{(\bar{\tau}_y)_n}{\tau_y^{(1)}} = \sqrt{c^{(1)}\left[1 - c^{(2)}\frac{1 - c^{(1)}(1 - 2S_{1212}^{(1)}(\alpha))(1 - \mu^{(1)}/\mu^{(2)})^2}{(1 - c^{(1)}(1 - \mu^{(1)}/\mu^{(2)})(1 - 2S_{1212}^{(1)}(\alpha)))^2}\right]^{-1}}. \tag{42}$$

We note that these expressions are independent of the material nonlinearity since they only serve to characterize the *initial* yield stress of the composite. On the other hand, they are dependent on the inclusion concentration $c^{(2)}$ and shape α, the stiffness ratio $\mu^{(1)}/\mu^{(2)}$ and the yield stress of the matrix material $\tau_y^{(1)}$. We further note that the above results approach the results of Li *et al.* (1992), for rigidly reinforced composites, in the limit as $\mu^{(1)}/\mu^{(2)} \to 0$.

5. RESULTS

In this section, we explore the effects of particle shape and stiffness on the effective constitutive behavior of the model metal-matrix composites discussed in the previous section. We will investigate, in particular, the effects of the inclusion aspect ratio α and stiffness ratio $\mu^{(1)}/\mu^{(2)}$ on the initial yield stresses under the three different loading modes, $(\bar{\tau}_y)_d$, $(\bar{\tau}_y)_p$ and $(\bar{\tau}_y)_n$, on the concomitant yield surfaces, and on the overall stress–strain relations.

We begin with Figs 2, showing the dependence of $(\bar{\tau}_y)_d$, $(\bar{\tau}_y)_p$ and $(\bar{\tau}_y)_n$ on α and $\mu^{(1)}/\mu^{(2)}$, as determined by relations (42). More specifically, Figs 2(a–c) give respectively, plots of (the reciprocals of) $(\bar{\tau}_y)_d$, $(\bar{\tau}_y)_p$ and $(\bar{\tau}_y)_n$, normalized by $\tau_y^{(1)}$, as functions of α (on a logarithmic scale), for four different values of $\mu^{(1)}/\mu^{(2)}$ ($= 0$, 0.06, 0.2 and 0.5) and a fixed value of $c^{(2)}$ ($= 0.2$). Thus, Fig. 2(a) shows that, for fixed *finite* $c^{(2)}$, the axisymmetric yield stress $(\bar{\tau}_y)_d$ of composites with prolate (oblate) inclusions increases monotonically with increasing (decreasing) aspect ratios. The extreme limits of the aspect ratio ($\alpha = 0$ and ∞), corresponding (as expected on physical grounds) to the cases of continuous reinforcement (laminates and fiber-reinforced composites, respectively) yield the largest values of $(\bar{\tau}_y)_d$. It is further observed that this reinforcing effect becomes significantly more marked with increasing inclusion stiffness (decreasing $\mu^{(1)}/\mu^{(2)}$), with prolate spheroids being somewhat more efficient in increasing the overall axisymmetric yield stress than oblate spheroids. In

contrast, it is also seen that nearly spherical particles have a relatively small effect on the overall axisymmetric yield stress of composites. In fact, as a function of α, the minimum strengthening effect for this loading mode takes place for α near 0.65. Figure 2(b) shows corresponding results for the overall transverse yield stress $(\tilde{\tau}_y)_p$. It is observed that in this case oblate inclusions are most efficient in increasing the transverse yield stress of the composite, whereas prolate inclusions are least efficient. These results are in agreement with our physical intuition, since the transverse shear behavior of the extreme cases of laminates and fiber-reinforced composites is expected to be controlled by the stiffer and weaker phases, respectively. For this mode (transverse shear), increasing inclusion stiffness (decreasing $\mu^{(1)}/\mu^{(2)}$) also has the effect of increasing the overall yield stress level, but this magnifying effect is only significant for oblate spheroids. On the other hand, Fig. 2(c) shows that the effect of both prolate and oblate inclusions is to reduce the longitudinal yield stress $(\tilde{\tau}_y)_n$ of the composite.
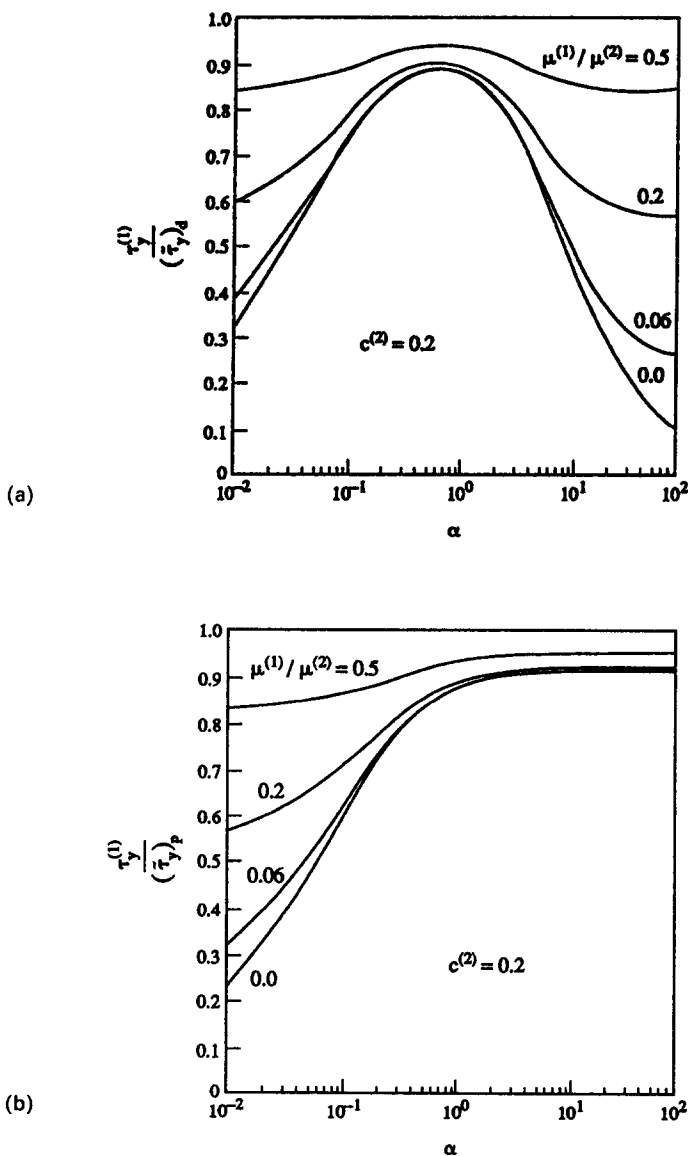

Fig. 2. The effect of inclusion shape α and stiffness ratio $\mu^{(1)}/\mu^{(2)}$ on the single-mode effective yield stresses of metal-matrix composites reinforced by aligned, spheroidal, linear-elastic inclusions in fixed proportion $c^{(2)}$. (a) Plot of $(\tilde{\tau}_y)_d$ (axisymmetric yield stress) versus α. (b) Plot of $(\tilde{\tau}_y)_p$ (transverse yield stress) versus α. (c) Plot of $(\tilde{\tau}_y)_n$ (longitudinal yield stress) versus α. (d) Plot of $(\tilde{\tau}_y)_d$ versus $\mu^{(1)}/\mu^{(2)}$.
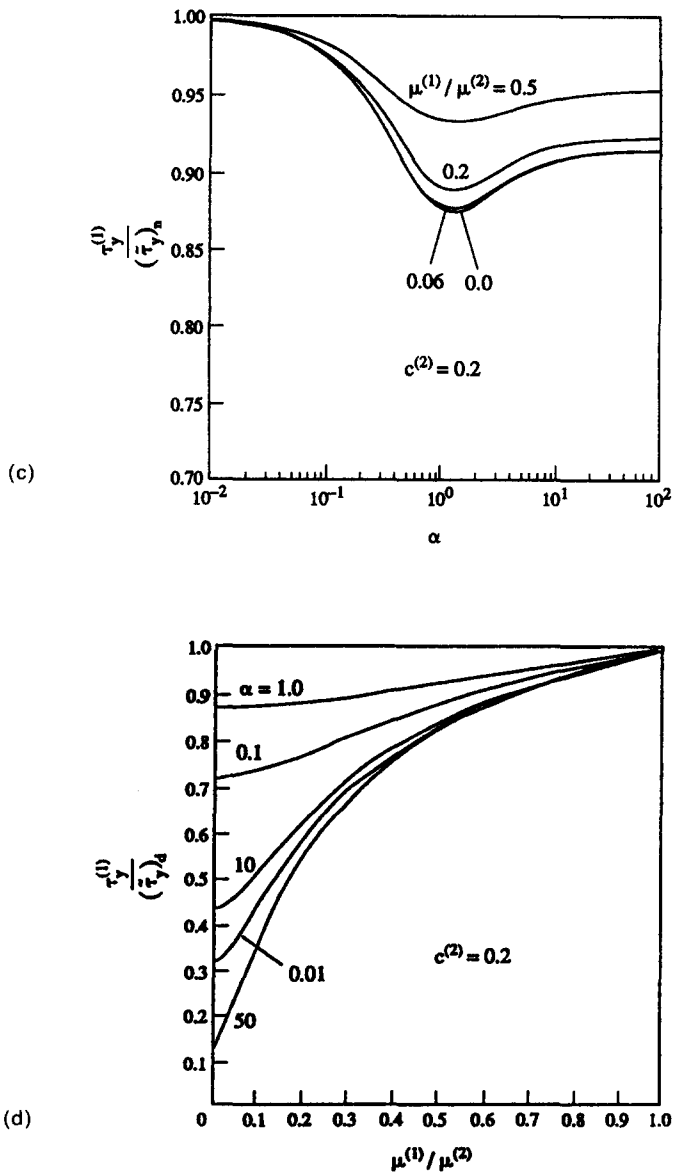
Fig. 2 (continued).

(These results can also be checked against our physical intuition by considering the extreme cases of laminates and fiber-reinforced composites.) In fact, slightly prolate inclusions with α near 1.4 result in the largest overall longitudinal yield stresses. In this case, increasing inclusion stiffness (decreasing $\mu^{(1)}/\mu^{(2)}$) does not have a significant effect in increasing the yield stress of the composite. We also note that the values of $(\tilde{\tau}_y)_p$ and $(\tilde{\tau}_y)_n$ in the limit as $\alpha \to \infty$ are identical, so that incompressible fiber-reinforced composites have identical yield stress values in the transverse and longitudinal shear modes. Finally, Fig. 2(d) shows plots of (the reciprocals of) $(\tilde{\tau}_y)_d$, normalized by $\tau_y^{(1)}$, versus the stiffness ratio $\mu^{(1)}/\mu^{(2)}$, for several values of α. These plots confirm our previous observations that increasing particle stiffness has the effect of increasing the axisymmetric yield stress of the composite, and that this effect is "synergistic" with the reinforcing effect produced by the selection of the limiting values of the aspect ratios for the inclusions. Thus, the combined effect of these two reinforcing mechanisms may lead to extremely high theoretical predictions for $(\tilde{\tau}_y)_d$. However, these predictions will not be realized in practice due to the presence of imperfections in the composite leading to localized, and eventually macroscopic, failure. Similar

plots may be obtained for the other two modes $(\tilde{\tau}_y)_p$ and $(\tilde{\tau}_y)_n$, except that the relative trends for curves with the same values of α [as in Fig. 2(d)] will be different for these two modes.

Figures 3 show plots of different cross-sections of the effective yield surfaces of the particle-reinforced composites, for fixed values of $c^{(2)}(=0.2)$ and $\mu^{(1)}/\mu^{(2)}$ $(=0.2)$, and several values of α $(=0.01, 0.1, 1, 10$ and $50)$. Figure 3(a) shows yield surfaces under combinations of $\tilde{\tau}_p$ and $\tilde{\tau}_d$. It is observed that these surfaces are smooth, and that the spheroidal particles provide between 10 and 75% additional reinforcement over the matrix yield stress level, for this class of composites. It is also clear that spherical particles provide the least amount of reinforcement for this combination of modes (except for a small sector near the pure transverse loading mode, where prolate spheroids lead to slightly smaller reinforcement). On the other hand, it appears that oblate spheroids provide greatest overall reinforcement (except near the pure axisymmetric mode, where prolate spheroids lead to
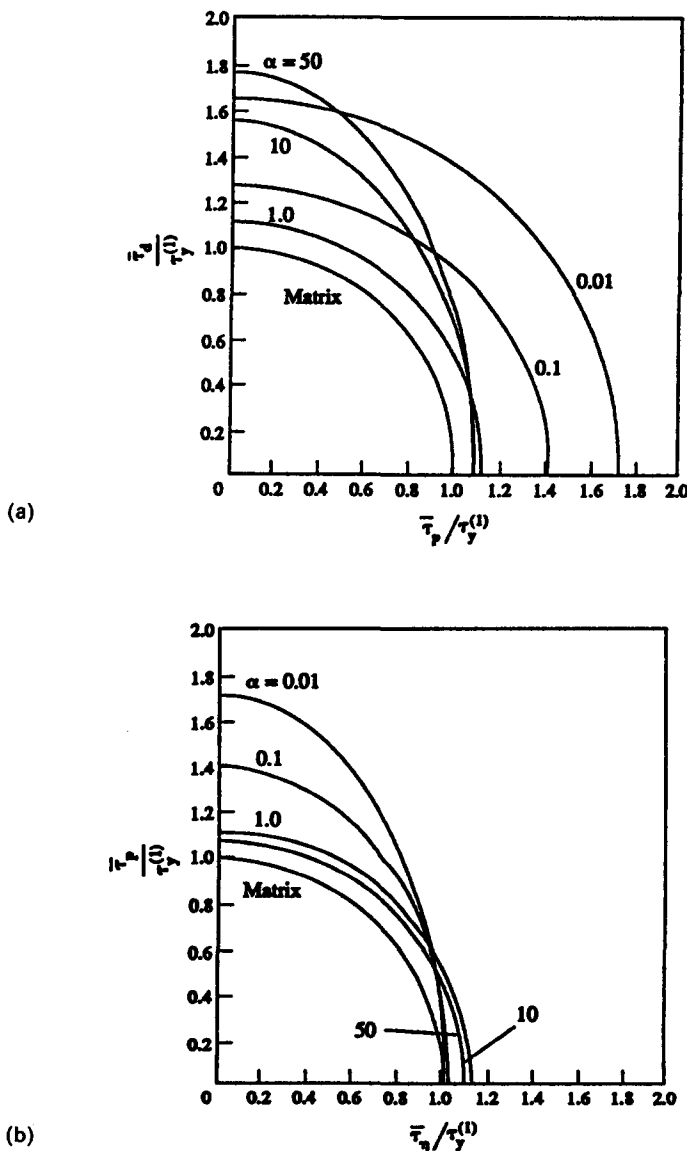

(a)

(b)

Fig. 3. Effective yield surfaces of the metal-matrix composites reinforced by algined inclusions with stiffness ratio $\mu^{(1)}/\mu^{(1)} = 0.2$, concentration $c^{(2)} = 0.2$, and varying aspect ratios. (a) Combined axisymmetric shear $\tilde{\tau}_d$ and transverse shear $\tilde{\tau}_p$. (b) Combined transverse shear $\tilde{\tau}_d$ and longitudinal shear $\tilde{\tau}_p$.

even greater reinforcement). Figure 3(b) shows the corresponding cross-sections of the yield surfaces under combined $\bar{\tau}_p$ and $\bar{\tau}_n$. Once again, it appears that for this loading combination oblate spheroids provide greatest overall reinforcement (except for nearly pure longitudinal stresses, for which oblate spheroids do worst and hardly improve on the matrix value). On the other hand, prolate shapes do worse than spherical shapes, which provide only about 10% isotropic reinforcement. The corresponding figure for combined $\bar{\tau}_n - \bar{\tau}_d$ loading is not shown, but the results demonstrate that prolate spheroids are generally best for this type of combined loading.

Figure 4 shows plots of the stress–strain relations, appropriately normalized, for the three pure loading modes, with a fixed value of $c^{(2)}(=0.2)$, two values of $\mu^{(1)}/\mu^{(2)}$ ($=0$ and 0.2), two values of n ($=3$ and 10) and several values of α ($=0.01, 0.1, 1, 10$ and 50). Figure 4(a) shows plots of $\bar{\tau}_d$ versus $\bar{\gamma}_d$, with $\mu^{(1)}/\mu^{(2)} = 0.2$ and $n = 3$, for the given values of α. The behavior of the matrix is also shown for comparison. It is observed that the overall stress–strain curves have the same general features as the matrix material, except that the load-carrying capacity of the composite is significantly increased, especially for the extreme values of α. It appears, however, that prolate inclusions lead to the greatest overall load-carrying capacity (several times higher than spherical inclusions, for example). Figure 4(b) shows the same set of plots for $\bar{\tau}_d$ versus $\bar{\gamma}_d$, for the same value of $\mu^{(1)}/\mu^{(2)}$, but a different value of n ($=10$). The general trends are similar to those of Figure 4(a), but the softening effect of the more ductile matrix phase is now more marked. Figure 4(c) gives results for the same set of parameters as Figure 4(b), except that the value of $\mu^{(1)}/\mu^{(2)}$ has been changed from 0.2 to 0 (corresponding to rigid inclusions). It is observed that the initial yielding of the composite occurs at much higher stresses, in agreement with our discussion of Figs 2(a) and (d), but the post-yielding behavior of the curves in Fig. 4(c) is very similar to those in Fig. 4(b), indicating that particle stiffness does have a significant effect on the post-yielding behavior of the composite (for strains greater than about five times the yield level). Figures 5(a, b) show plots of $\bar{\tau}_p$ versus $\bar{\gamma}_p$, for $\mu^{(1)}/\mu^{(2)} = 0.2$ and for $n = 3$ and 10, respectively. It is observed that the plots are similar in character to the corresponding plots in Figs 4(a, b) for the same sets of parameters. However, for this loading mode, it appears that oblate inclusions are by far most effective in increasing the load-carrying capacity of the composite. In fact, prolate inclusions result in slightly lower stress–strain relations than spherical inclusions. Although the results are not shown, corresponding plots for rigid inclusions demonstrate that the stiffness of the particle only has a significant effect near the yield point of the composite, but this effect quickly disappears as the plastic deformation progresses. Finally, Figs 6(a, b) show plots of $\bar{\tau}_n$ versus $\bar{\gamma}_n$, for the usual values of the material parameters. The main observation relating to these plots is that particle shape does not seem to affect very significantly the load-carrying capacity of the composite in this loading mode. In fact, both oblate and prolate shapes tend to diminish the load-carrying capacity of the composite, when compared with nearly spherical inclusions.

6. CONCLUDING REMARKS

This study has dealt with the effects of particle shape and stiffness on the effective constitutive behavior of metal-matrix composites reinforced by stiff spheroidal inclusions with linear-elastic properties. Many other relevant effects, including those arising from residual stresses, cavitation and interfacial cracks (between the inclusion and matrix phases), have therefore been neglected in the interest of simplicity. Although several papers have appeared recently (as discussed in the Introduction) dealing with numerical analysis of the response of this class of materials to *axisymmetric* loading conditions, the present work appears to be among the first [see also Talbot and Willis (1992) and Zhao and Weng (1990)] to deal with *general* loading conditions, including transverse and longitudinal shear loading. It is found that the effects of particle shape and stiffness depend strongly on the loading mode. Thus, prolate shapes lead to the largest increases in the yield stress and load-carrying capacity of this class of composites when subjected to axisymmetric loading; oblate shapes lead to large increments in the yield stress and load-carrying capacity of the composites for both the transverse shear and axisymmetric shear modes; and nearly spherical shapes
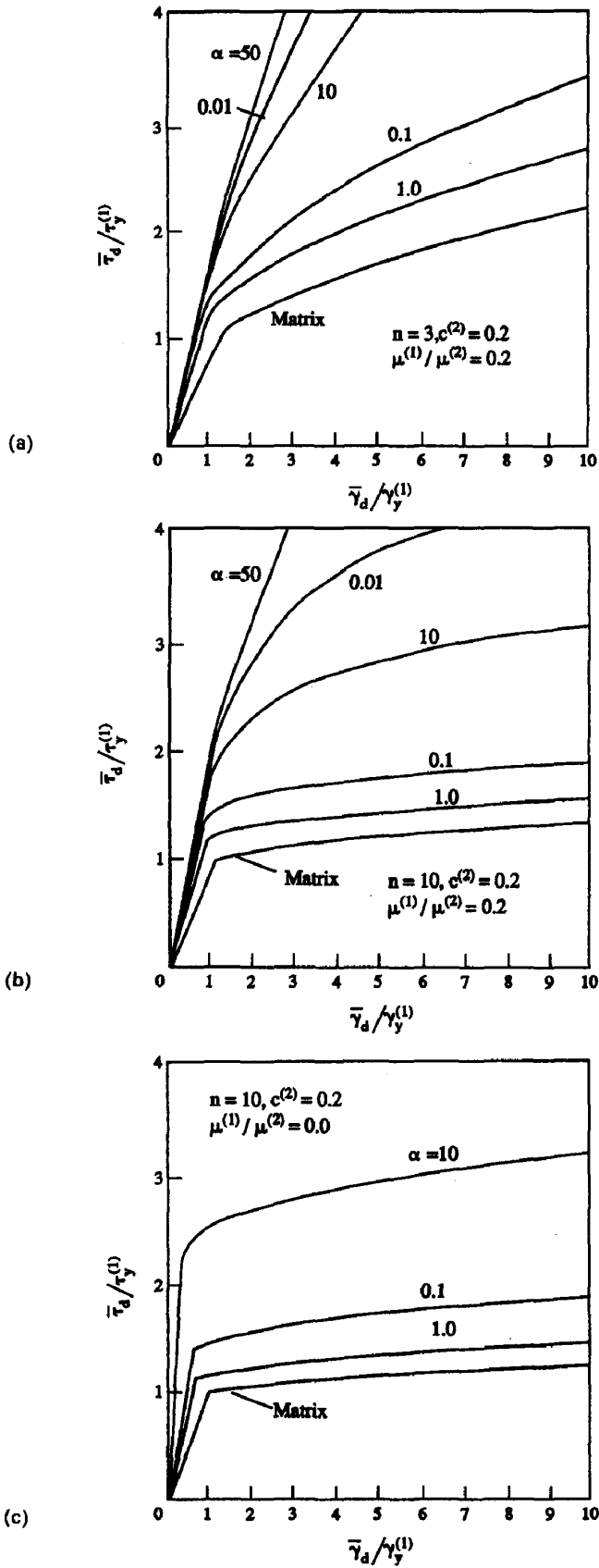
Fig. 4. Axisymmetric effective stress–strain relations ($\bar{\tau}_d$ versus $\bar{\gamma}_d$) for the particle-reinforced, metal-matrix composite, with inclusion concentration $c^{(2)} = 0.2$, and several values of the aspect ratio α. The stiffness ratio is $\mu^{(1)}/\mu^{(2)} = 0.2$ for (a) and (b), and 0 for (c). The matrix hardening exponent is (a) $n = 3$, (b) $n = 10$, (c) $n = 10$.
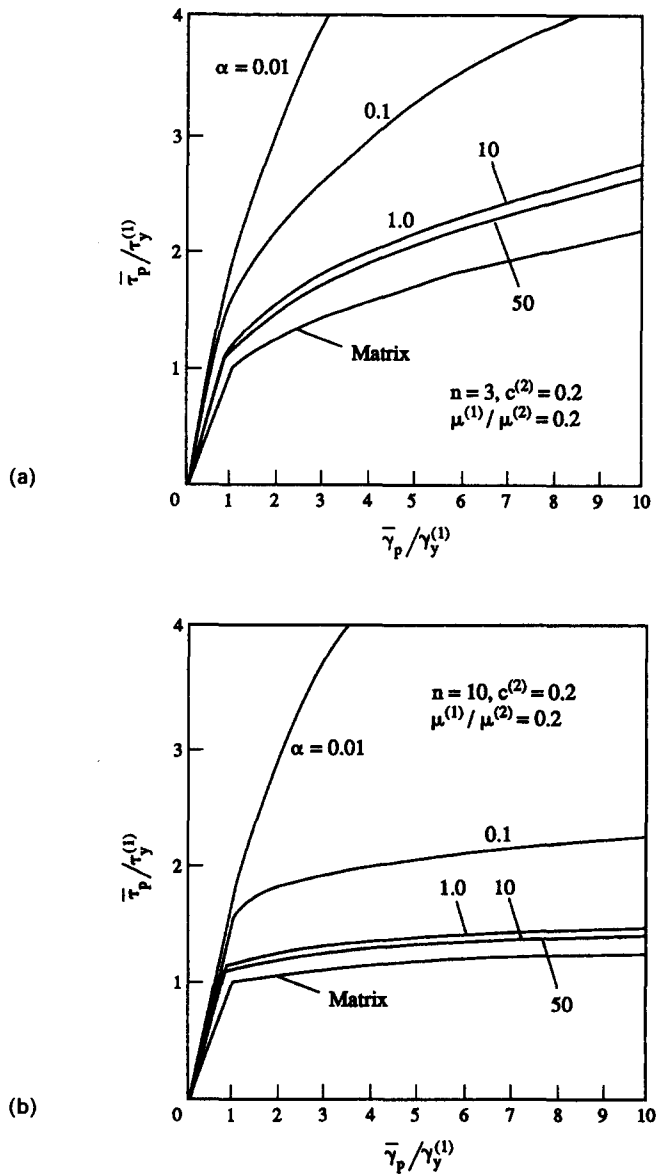
Fig. 5. Transverse effective stress–strain relations ($\bar{\tau}_p$ versus $\bar{\gamma}_p$) for the particle-reinforced, metal-matrix composite, with inclusion concentration $c^{(2)} = 0.2$, stiffness ratio $\mu^{(1)}/\mu^{(2)} = 0.2$, and several values of the aspect ratio α. The matrix hardening exponent is (a) $n = 3$, (b) $n = 10$.

provide the optimal amount of reinforcement for the longitudinal mode, although this reinforcement is actually quite modest in size. The large reinforcing effects of the prolate and oblate shapes for the axisymmetric and transverse modes, respectively, can be best understood by recognizing that, at *finite* concentrations of inclusions, the limiting values of the aspect ratio correspond to continuous reinforcement (laminates and fiber-reinforced composites, respectively). Very different results would be obtained if the extreme limits of aspect ratio were considered with fixed inclusion density, instead of fixed inclusion volume fraction [see Talbot and Willis (1992) and Li et al. (1993)]. In addition, it is found that increasing particle stiffness leads to concomitant increases in the load-carrying capacity of the composite, with larger, synergistic, increases for the particle shapes with extreme values of the aspect ratio. These results are expected to be of significance in the design of optimal microstructures for particle-reinforced, metal-matrix composites. Finally, it should be mentioned that a limitation of the present results, which prevented a quantitative comparison
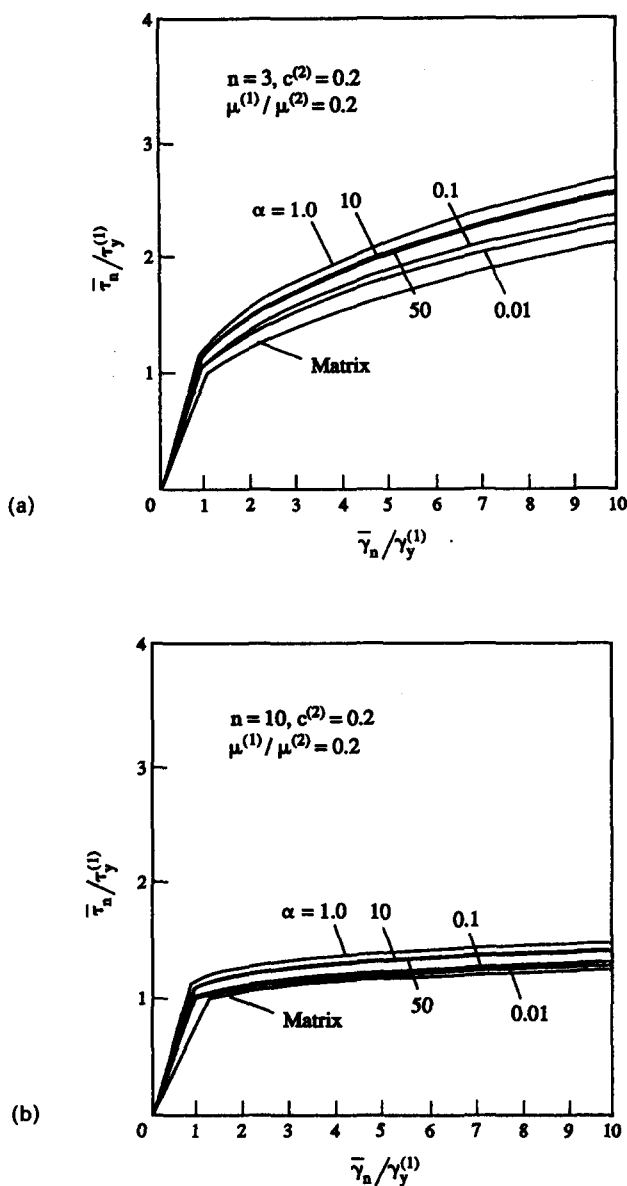
Fig. 6. Longitudinal effective stress–strain relations ($\bar{\tau}_n$ versus $\bar{\gamma}_n$) for the particle-reinforced, metal-matrix composite, with inclusion concentration $c^{(2)} = 0.2$, stiffness ratio $\mu^{(1)}/\mu^{(2)} = 0.2$, and several values of the aspect ratio α. The matrix hardening exponent is (a) $n = 3$, (b) $n = 10$.

with the numerical results available for periodic composites, is that the phases of the composites were assumed to be incompressible. However, this limitation can be eliminated at the cost of complicating the analyses; this is presently being pursued.

REFERENCES

Accorsi, M. L. and Nemat-Nasser, S. (1986). Bounds on the overall elastic and instantaneous elastoplastic moduli of periodic composites. *Mech. Mater.* **5**, 209–220.
Bao, G., Hutchinson, J. W. and McMeeking, R. M. (1991). Particle reinforcement of ductile matrices against plastic flow and creep. *Acta Metall. Mater.* **39**, 1871–1882.
deBotton, G. and Ponte Castañeda, P. (1992). On the ductility of laminated materials. *Int. J. Solids Structures* **29**, 2329–2353.

deBotton, G. and Ponte Castañeda, P. (1993). Elastoplastic constitutive relations for fiber-reinforced solids. *Int. J. Solids Structures* **30**(14), 1865–1890.

Budiansky, B. (1959). A reassessment of deformation theories of plasticity. *J. Appl. Mech.* **26**, 259–264.

Budiansky, B. (1965). On the elastic moduli of some heterogeneous materials. *J. Mech. Phys. Solids* **13**, 223–227.

Christensen, R. M. and Lo, K. H. (1979). Solutions for effective shear properties in three phase sphere and cylinder models. *J. Mech. Phys. Solids* **27**, 315–330.

Christman, T., Needleman, A. and Suresh, S. (1989). An experimental and numerical study of deformation in metal-ceramic composites. *Acta Metall.* **37**, 3029–3050.

Drucker, D. C. (1965). Engineering and continuum aspects of high strength materials. In *High Strength Materials* (Edited by V. F. Zackey), pp. 795–833. Wiley, New York.

Drucker, D. C. (1966). The continuum theory of plasticity on the macroscale and the microscale. *J. Mater.* **1**, 873–910.

Duva, J. M. (1984). A self-consistent analysis of the stiffening effect of rigid inclusions on a power-law material. *J. Engng Mater. Technol.* **106**, 317–321.

Eshelby, J. D. (1957). The determination of the elastic field of an ellipsoidal inclusion, and related problems. *Proc. Roy. Soc. Lond. A* **241**, 376–396.

Francfort, G. and Murat, F. (1986). Homogenization and optimal bounds in linear elasticity. *Arch. Rat. Mech. Anal.* **94**, 307–334.

Hashin, Z. (1965). On elastic behavior of fiber reinforced materials of arbitrary transverse phase geometry. *J. Mech. Phys. Solids* **13**, 119–134.

Hashin, Z. and Shtrikman, S. (1962). On some variational principles in anisotropic and nonhomogeneous elasticity. *J. Mech. Phys. Solids* **10**, 335–342.

Hashin, Z. and Shtrikman, S. (1963). A variational approach to the theory of the elastic behavior of multiphase materials. *J. Mech. Phys. Solids* **11**, 127–140.

He, M. Y. (1990). On the flow and creep strength of power-law materials containing rigid reinforcements. *Mater. Res. Soc. Symp. Proc.* **194**, 15–22.

Hill, R. (1963). Elastic properties of reinforced solids: Some theoretical principles. *J. Mech. Phys. Solids* **11**, 357–372.

Hill, R. (1964). Theory of mechanical properties of fiber-strengthened materials—I. Elastic behavior. *J. Mech. Phys. Solids* **12**, 199–213.

Hill, R. (1965). A self-consistent mechanics of composite materials. *J. Mech. Phys. Solids* **13**, 213–222.

Hom, C. L. (1992). Three-dimensional finite element analysis of plastic deformation in a whisker-reinforced metal matrix composite. *J.Mech. Phys. Solids* **40**, 991–1008.

Lee, B. J. and Mear, M. E. (1991a). Effect of inclusion shape on the stiffness of nonlinear two-phase composites. *J. Mech. Phys. Solids* **39**, 627–649.

Lee, B. J. and Mear, M. E. (1991b). Effect of inclusion shape on stiffness of isotropic and transversely isotropic two-phase composites. *Int. J. Solids Structures* **28**, 975–1001.

Li, G., Ponte Castañeda, P. and Douglas, A. S. (1993). Constitutive models for ductile solids reinforced by rigid spheroidal inclusions. *Mech. Mater.* **15**, 279–300.

Lipton, R. (1991). On the behavior of elastic composites with transverse isotropic symmetry. *J. Mech. Phys. Solids* **39**, 663–681.

Mori, T. and Tanaka, K. (1973). Average stress in matrix and average elastic energy of materials with misfitting inclusions. *Acta Metall.* **21**, 571–574.

Ponte Castañeda, P. (1991a). The effective mechanical properties of nonlinear isotropic composites. *J. Mech. Phys. Solids* **39**, 45–71.

Ponte Castañeda, P. (1991b). The effective properties of brittle/ductile incompressible composites. In *Inelastic Deformation of Composite Materials* (Edited by G. J. Dvorak), pp. 215–231.

Ponte Castañeda, P. (1992). New variational principles in plasticity and their application to composite materials. *J. Mech. Phys. Solids* **40**, 1757–1788.

Ponte Castañeda, P. and Willis, J. R. (1988). On the overall properties of nonlinearly viscous composites. *Proc. Roy. Soc. Lond. A* **416**, 217–244.

Suquet, P. (1992a). On bounds for the overall potential of power law materials containing voids with arbitrary shape. *Mech. Res. Comm.* **19**, 51–58.

Suquet, P. (1992b). Sur le comportment mecanique macroscopique de composites non lineares. *C. R. Acad. Sci. Paris, Serie II* **315**, 909–914.

Suquet, P. (1993). Overall potentials and extremal surfaces of power-law, or ideally plastic components. *J. Mech. Phys. Solids* **41**, 981–1002.

Talbot, D. R. S. and Willis, J. R. (1985). Variational principles for nonlinear inhomogeneous media. *IMA J. Appl. Math.* **35**, 39–54.

Talbot, D. R. S. and Willis, J. R. (1992). Some simple explicit bounds for the overall behavior of nonlinear composites. *Int. J. Solids Structures* **29**, 1981–1987.

Tandon, G. P. and Weng, G.J. (1988). A theory of particle-reinforced plasticity. *J. Appl. Mech.* **55**, 126–135.

Teply, J. L. and Dvorak, G.J. (1988). Bounds on the overall instantaneous properties of elastic-plastic composites. *J. Mech. Phys. Solids* **36**, 29–58.

Tvergaard, V. (1990). Analysis of tensile properties for a whisker-reinforced metal-matrix composite. *Acta Metall. Mater.* **38**, 185–194.

Walpole, L. J. (1966). On bounds for the overall elastic moduli of inhomogeneous systems—Parts I and II. *J. Mech. Phys. Solids* **14**, 151–262; 289–301.

Walpole, L. J. (1969). On the overall elastic moduli of composite materials. *J. Mech. Phys. Solids* **17**, 235–251.

Weng, G. J. (1992). Explicit evaluation of Willis' bounds with ellipsoidal inclusions. *Int. J. Engng Sci.* **30**, 83–92.

Willis, J. R. (1977). Bounds and self-consistent estimates for the overall moduli of anisotropic composites. *J. Mech. Phys. Solids* **25**, 185–202.

Willis, J. R. (1980). Relationships between derivations of the overall properties of composites by perturbation

expansions and variational principles. In *Variational Methods in Mechanics of Solids* (Edited by S. Nemat-Nasser), pp. 59–66. Pergamon Press, Oxford.

Willis, J. R. (1981). Variational and related methods for the overall properties of composites. In *Advances in Applied Mechanics* (Edited by C. S. Yih), pp. 1–48. Academic Press, New York.

Willis, J. R. (1991). On methods for bounding the overall properties of nonlinear composites. *J. Mech. Phys. Solids* **39**, 73–86.

Zhao, Y. H. and Weng, G. J. (1990). Theory of plasticity for a class of inclusion and fiber-reinforced composites. In *Micromechanics and Inhomogeneity* (Edited by G. J. Weng, M. Taya and H. Abe), pp. 599–622. Springer, New York.

APPENDIX

For a spheroidal inclusion, aligned with the x_1 axis, the components of the Eshelby's tensor are (Eshelby, 1957)

$$S^{(1)}_{1111} = \frac{1}{2(1-v^{(1)})} \left\{ 1 - 2v^{(1)} + \frac{3\alpha^2 - 1}{\alpha^2 - 1} - \left[1 - 2v^{(1)} + \frac{3\alpha^2}{\alpha^2 - 1} \right] g \right\},$$

$$S^{(1)}_{2222} = \frac{3}{8(1-v^{(1)})} \frac{\alpha^2}{\alpha^2 - 1} + \frac{1}{4(1-v^{(1)})} \left[1 - 2v^{(1)} - \frac{9}{4(\alpha^2 - 1)} \right] g,$$

$$S^{(1)}_{3333} = S^{(1)}_{2222},$$

$$S^{(1)}_{2233} = \frac{1}{4(1-v^{(1)})} \left\{ \frac{\alpha^2}{2(\alpha^2 - 1)} - \left[1 - 2v^{(1)} + \frac{3}{4(\alpha^2 - 1)} \right] g \right\},$$

$$S^{(1)}_{3322} = S^{(1)}_{2233},$$

$$S^{(1)}_{2211} = - \frac{1}{2(1-v^{(1)})} \frac{\alpha^2}{\alpha^2 - 1} + \frac{1}{4(1-v^{(1)})} \left\{ \frac{3\alpha^2}{\alpha^2 - 1} - (1 - 2v^{(1)}) \right\} g,$$

$$S^{(1)}_{3311} = S^{(1)}_{2211},$$

$$S^{(1)}_{1122} = \frac{1}{2(1-v^{(1)})} \left\{ -1 + 2v^{(1)} - \frac{1}{\alpha^2 - 1} + \left[1 - 2v^{(1)} + \frac{3}{2(\alpha^2 - 1)} \right] g \right\},$$

$$S^{(1)}_{1133} = S^{(1)}_{1122},$$

$$S^{(1)}_{1212} = \frac{1}{4(1-v^{(1)})} \left\{ 1 - 2v^{(1)} - \frac{\alpha^2 + 1}{\alpha^2 - 1} - \frac{1}{2} \left[1 - 2v^{(1)} - \frac{3(\alpha^2 + 1)}{\alpha^2 - 1} \right] g \right\},$$

$$S^{(1)}_{1313} = S^{(1)}_{1211},$$

$$S^{(1)}_{2323} = \frac{S^{(1)}_{2222} - S^{(1)}_{2233}}{2}, \tag{A1}$$

where $v^{(1)}$ is the Poisson's ratio of the matrix material, $\alpha = b/a$ is the aspect ratio of the spheroidal inclusion (see Fig.1), and f and g are given respectively by

$$f(\alpha) = \frac{2\alpha^2 + 1}{\alpha^2 - 1} \left[\tfrac{3}{2} g(\alpha) - 1 \right] \tag{A2}$$

and

$$g(\alpha) = \frac{\alpha}{(\alpha^2 - 1)^{3/2}} [\alpha(\alpha^2 - 1)^{1/2} - \cosh^{-1} \alpha], \quad \alpha > 1, \quad \text{prolate,}$$

$$\frac{\alpha}{(1 - \alpha^2)^{3/2}} [\cos^{-1} \alpha - \alpha(1 - \alpha^2)^{1/2}], \quad \alpha < 1, \quad \text{oblate.} \tag{A3}$$